JACS
JOURNAL OF THE AMERICAN CHEMICAL SOCIETY

pubs.acs.org/JACS Article

Formation of the End-on Bound Lanthanide Dinitrogen Complexes [R2N)3Ln N N Ln NR2)3]2 from Divalent [R2N)3Ln]1 Salts R = SiMe3)

Austin J. Ryan Sree ganesh Balasubramani Joseph W. Ziller Filipp Furche and William J. Evans

Cite This: J Am Chem Soc 2020 142 9302 9313 Read Online

CCESS | Metrics More | Article Recommendations | Supporting Information

ABSTRACT: Lanthanide-based dinitrogen reduction chemistry has been expanded by the discovery of the rst end-on Ln_2(-η^1:η^1-N_2) complexes, whose synthesis and reactivity help explain the reduction of N_2 by the combination of trivalent $Ln(NR_2)_3$ complexes (R = $SiMe_3$) and potassium. The formation of end-on versus the more common side-on Ln_2(-η^2:η^2-N_2) complexes is possible by using recently discovered Ln(II) complexes ligated by three NR_2 amide ligands (R = $SiMe_3$). The isolated Ln(II) tris(amide) complex [K(crypt)][Tb(NR_2)$_3$] (crypt = 2.2.2-cryptand), **1-Tb**, reacts with dinitrogen in Et_2O at 35 °C to form the end-on bridging dinitrogen complex [K(crypt)]$_2${[(R_2N)$_3$Tb]$_2$[-η^1:η^1-N_2]}, **2-Tb**. The 18-crown-6 (18-c-6) Tb(II) analogue, [K(18-c-6)$_2$][Tb(NR_2)$_3$], **3-Tb**, also reacts with N_2 to form an end-on product, [K_2(18-c-6)$_3$]{[(R_2N)$_3$Tb]$_2$[-η^1:η^1-N_2]}, **4-Tb**. The reaction of **1-Gd** with dinitrogen forms a complex with the same composition as **2-Tb** but with both side-on and end-on bonding of the N_2 unit in the same crystal, [K(crypt)]$_2${[(R_2N)$_3$Gd]$_2$[-η^x:η^x-N_2]} (x = 1 and 2), **5-Gd**. Similarly, the 18-c-6 Gd(II) complex, **3-Gd**, generates a product with both binding modes: [K_2(18-c-6)$_3$]{[(R_2N)$_3$Gd]$_2$[-η^x:η^x-N_2]} (x = 1, 2), **6-Gd**. All of these new reduced dinitrogen complexes, **2-Tb**, **4-Tb**, **5-Gd**, and **6-Gd**, have three ancillary amide ligands per metal. In contrast, the side-on bound complexes, [(THF)(R_2N)$_2$Ln]$_2$[-η^2:η^2-N_2], **7-Ln**, observed previously in Ln(NR_2)$_3$/K/N_2 reactions, have only two amides per metal. A connection between these systems related to their formation was observed in the structure of the bimetallic penta-amide complex, [K(THF)$_6$]{[(THF)(R_2N)$_2$Gd][-η^2:η^2-N_2][Gd(NR_2)$_3$]}, **8-Gd**, synthesized at 196 °C. Reaction conditions are crucial in this dinitrogen reaction system. When **5-Gd** and **6-Gd** are warmed above 15 °C, they reform Gd(II) complexes. If **1-Gd** is dissolved in THF instead of Et_2O under N_2, the irreversible formation of an $(N_2)^3$ complex [K(crypt)][(THF)(R_2N)$_2$Gd]$_2$[-η^2:η^2-N_2], **9-Gd**, is observed.

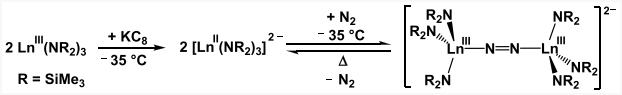

INTRODUCTION

The rst reduced-dinitrogen complex containing a rare-earth metal, [(C_5Me_5)$_2$Sm]$_2$[-η^2:η^2-N_2], was reported in 1988, eq 1,

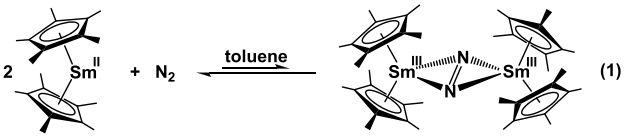

and had a planar side-on η^2-N_2 binding mode that had never been seen before in M_2N_2 dinitrogen complexes involving any metal.[1] Since that initial discovery, dozens of Ln_2N_2 (Ln = rare-earth metal, i.e. Sc, Y, and lanthanides) complexes have been isolated, and all of the lanthanide compounds display side-on -η^2:η^2-N_2 bonding, eq 2.[2] [18] These reactions differed from eq 1 in that the starting material was not a Ln(II) complex, but a combination of a Ln(III) starting material and potassium. Because molecular Ln(II) complexes for many of the metals in eq 2 were unknown when the dinitrogen reduction was discovered, the mode of formation of the (N N)^2 products was not obvious. The general formula of the (N N)^2 complexes in eq 2 is [A_2(THF)$_x$Ln^{III}]$_2$[-η^2:η^2-N_2] (x = 1, 2),

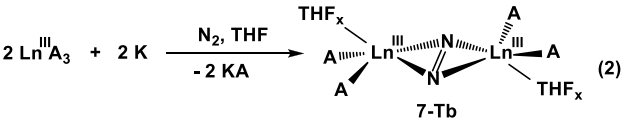

Ln = Sc, Y, La, Ce, Pr, Nd, Gd, Tb, Dy, Ho, Er, Tm, Lu
A = N($SiMe_3$)$_2$, $OC_6H_3{}^tBu_2$-2,6, C_5Me_5, C_5Me_4H, $C_5H_4SiMe_3$
x = 1, 2

where A is an anion, i.e. these are neutral complexes of Ln(III) ions with two anionic ligands on the metal in addition to the side-on bound (N N)^2 bridge. Bimetallic lanthanide complexes of the radical trianion $(N_2)^3$ [19] and the radical dianion $(NO)^2$ [20] have also been isolated with this planar side-on bonding mode, Figure 1.

Received: January 30, 2020
Published: March 29, 2020

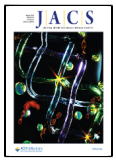

https://dx.doi.org/10.1021/jacs.0c01021
J Am Chem Soc 2020 142 9302 9313

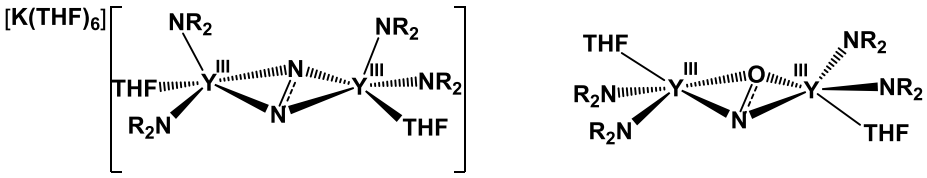

Figure 1. Side-on binding mode of the rst $(N_2)^3$ and $(NO)^2$ complexes.[19,20]

Hence, it was surprising to nd that the Sc(II) amide complex, $[Sc^{II}(NR_2)_3]^1$, reacts with N_2 to make an end-on reduced dinitrogen complex, $[K(crypt)]_2\{[(R_2N)_3Sc]_2[\ -\eta^1{:}\eta^1\text{-}N_2]\}$ (crypt = 2.2.2-cryptand), eq 3.[21] Generally, if Sc displays

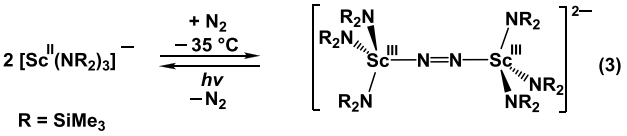

chemistry different from the other rare-earths, it is rationalized by the fact that scandium is much smaller. Based on the ionic radius, Sc would be 23rd in the series by size following the 0.013 Å average decrease from one lanthanide to the next. However, this scandium complex differed from the examples in eq 2 in that it retained all three $(NR_2)^1$ ligands. If steric crowding was an issue, it might be expected that a complex with two anionic amide ligands per metal would be found as in eq 2. On the other hand, the small size of scandium provides a higher charge-to-radius ratio and the increased Lewis acidity could help retain all three amides. The presence of a chelating agent for the K^{1+} countercation in eq 3 could also be important. Loss of $(NR_2)^1$ could be easier with an unchelated K^{1+} vs $[K(crypt)]^{1+}$. This has been observed in other systems such as the $\{U[N(CH_2CH_2NSiiPr_3)_3](NCO)][K(B15\text{-}c\text{-}5)_2$ (B15-c-5 = benzo-15-crown-5 ether) complex, which retained an NCO^1 ligand when the K^{1+} countercation was chelated with B15-c-5 but lost the NCO^1 ligand to form KNCO if no chelates were present.[22]

Once $[K(crypt)]_2\{[(R_2N)_3Sc]_2[\ -\eta^1{:}\eta^1\text{-}N_2]\}$ was identi ed, it was of interest to determine if end-on dinitrogen complexes of other rare earth metals could be made from Ln(II) precursors as shown in eq 3. Normally, yttrium, the congener of Sc, would be examined next because the Y(III) product would be diamagnetic. However, isolation of the Y(II) precursor, $[Y^{II}(NR_2)_3]^1$, has proven to be much more difficult than isolation of $[Sc^{II}(NR_2)_3]^1$.[23] However, $[Ln(NR_2)_3]^1$ complexes of the late lanthanides, Ln = Gd, Tb, Dy, Ho, and Er, are available.[24] This was surprising, because traditionally, Y(III) has been a good model for trivalent lanthanides of similar size, i.e. Ho(III) and Er(III). However, the data to date suggest that Y(II) may not be analogous to either Sc(II) or the late lanthanide +2 ions.[24 26]

To further explore the unusual chemistry in eq 3, we have examined dinitrogen reduction chemistry using $[Ln(NR_2)_3]^1$ complexes of the late lanthanides. We have chosen the two most stable members of this series, Ln = Gd and Tb,[23,24] and report here that they also can form end-on dinitrogen complexes with three amides per metal like scandium. These are the rst reduced dinitrogen complexes of lanthanides that feature end-on binding modes of the N_2 units. In addition, these reactions can also form dianionic side-on complexes with three amides per metal in single crystals containing both end-on and side-on bound dinitrogen ligands. The new $\{[(R_2N)_3Ln]_2[\ -\eta^x{:}\eta^x\text{-}N_2]\}^2$ dianions are potent reductants and can revert back to the highly reactive Tb(II) and Gd(II) complexes, $[Ln^{II}(NR_2)_3]^1$, a reaction not observed for other (N N)^2 complexes of Tb and Gd. The isolation of both end-on and side-on species in the same crystal as well as identi cation of a ve amide THF-solvated bimetallic side-on $\{[(THF)(R_2N)_2Gd][\ -\eta^2{:}\eta^2\text{-}N_2]\text{-}[Gd(NR_2)_3]\}^1$ monoanion suggest an explanation for the reaction chemistry in eq 2 that led to the neutral THF adducts $[(R_2N)_2(THF)_xLn]_2[\ -\eta^2{:}\eta^2\text{-}N_2]$.

This reaction chemistry is highly dependent on speci c reaction conditions, including solvent, temperature, and the speci c lanthanide involved. Reactions of complexes with crypt chelated potassium counter-cations are reported as well as compounds with 18-crown-6 (18-c-6) as the chelating agent.

RESULTS

A Pure End-on Ln N N Ln Complex. When crystalline samples of dark blue $[K(crypt)][Tb(NR_2)_3]$, **1-Tb**, originally prepared in an argon-containing glovebox, are dissolved in Et_2O prechilled to 35 °C in a nitrogen-containing glovebox, the dark color disappears within 5 min as the solvent is swirled in the vial. After the resulting yellow solution is kept at 35 °C overnight, single crystals of $[K(crypt)]_2\{[(R_2N)_3Tb]_2[\ -\eta^1{:}\eta^1\text{-}N_2]\}$, **2-Tb**, can be isolated, eq 4. The reported 10 20 yield on this highly

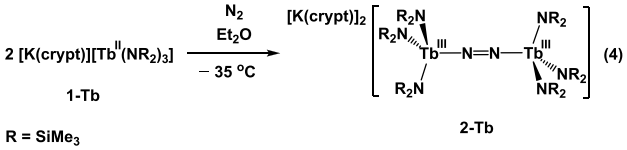

paramagnetic Tb(III) complex is low because we only claim a yield on samples of crystalline material that has been analyzed by X-ray crystallography. The reaction appears to proceed even faster at 78 °C (vide infra).

X-ray crystallography revealed that the reduced dinitrogen unit in **2-Tb** is bound end-on, as shown in Figure 2. Previously, all crystallographically characterized Ln_2N_2 complexes of the lanthanide metals have had side-on bound structures.[2 13] Only with scandium, eq 3, was an end-on structure found.[21]

The 1.217(3) Å N N bond length in **2-Tb** is within error of the 1.221(3) Å value in $[K(crypt)]_2\{[(R_2N)_3Sc]_2[\ -\eta^1{:}\eta^1\text{-}N_2]\}$, **2-Sc**,[21] and is consistent with a double bond, i.e. (N N)^2 .[27] This value is slightly smaller than the (N N)^2 distance of 1.271(4) Å measured in the side-on bound $[(R_2N)_2(THF)\text{-}Tb]_2(\ -\eta^2{:}\eta^2\text{-}N_2)$,[9] **7-Tb**, although there is considerable variation in N N distances depending on the quality of the crystal and the method of crystallization.[28]

The Tb N(N_2) average distance in **2-Tb**, 2.189(2) Å, is shorter than the Tb N(N_2) distances found in **7-Tb**, 2.301(2) and 2.328(2) Å. The Tb N(N_2) distance in **2-Tb** is signi cantly shorter than the Tb N(NR_2) distance which averages 2.326(6) Å and is similar to the Tb N(NR_2) distances observed in **7-Tb**, 2.301(2) and 2.328(2) Å.[9] The Tb metal centers in **2-Tb** deviate from the plane of the three amide nitrogen donor atoms by 0.663

https://dx.doi.org/10.1021/jacs.0c01021
J Am Chem Soc 2020 142 9302 9313

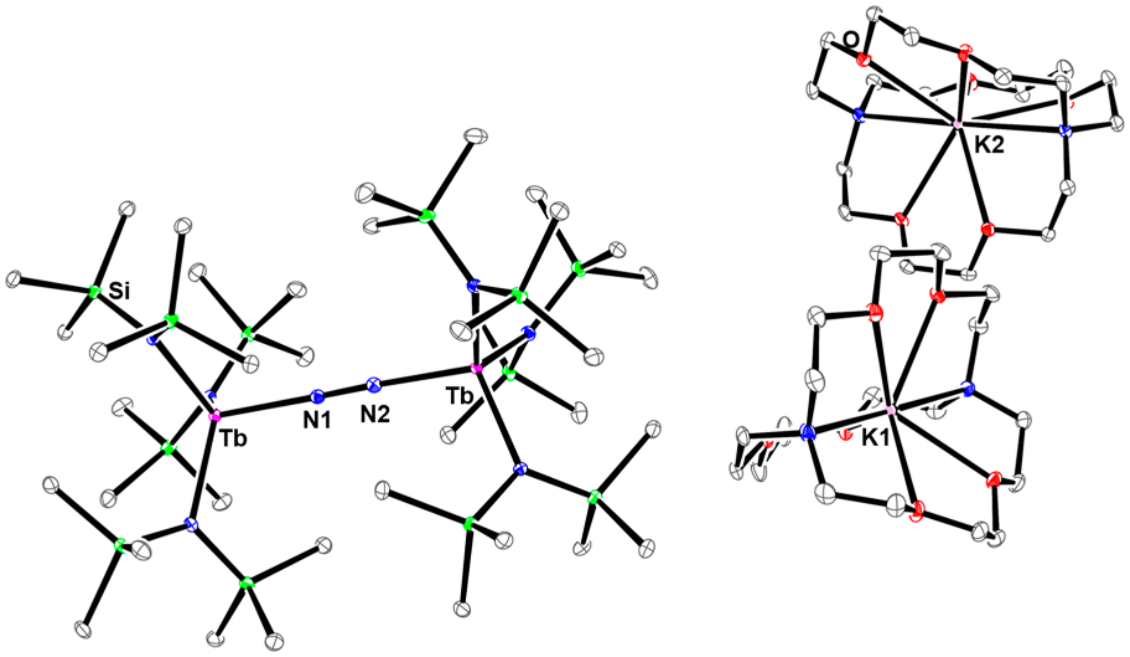

Figure 2. ORTEP representation of **2-Tb** drawn at the 50 probability level. Hydrogen atoms and Et_2O molecules have been excluded for clarity (O = red, N = blue, Si = green, C = gray).

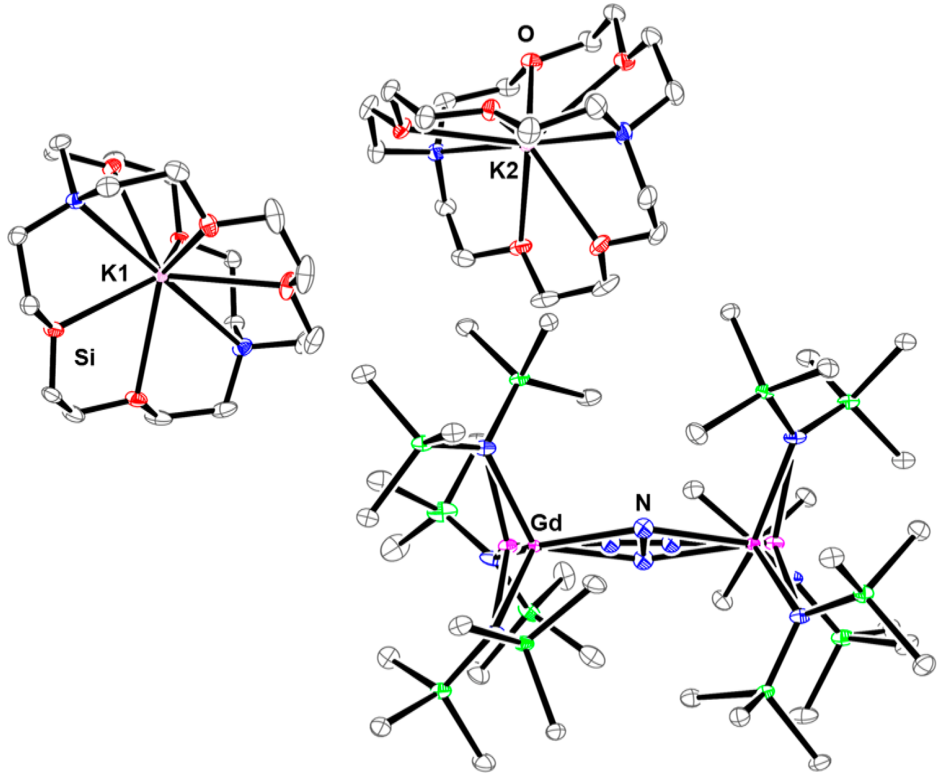

Figure 3. ORTEP representation of **5-Gd** drawn at the 50 probability level. Hydrogen atoms and Et_2O molecules excluded for clarity (O = red, N = blue, Si = green, Gd = plum, C = gray).

Å. In comparison, Tb is out of the plane by 0.604 Å in $Tb(NR_2)_3$,[29] 0.503 Å in $[K(crypt)][Tb(NR_2)_3]$, **1-Tb**,[24] and 0.201 Å in $[K(18\text{-c-}6)][Tb(NR_2)_3]$.[23] Tb is 0.629 Å out of the $N(NR_2)N(NR_2)O(THF)$ plane in **7-Tb**.[10]

The reaction between Tb(II) and N_2 was also examined with a complex containing 18-c-6 rather than crypt as the chelate for the potassium countercation of the $[Tb(NR_2)_3]^1$ anion. Differences in reactivity previously have been observed between 18-c-6 and crypt complexes of Ln(II) complexes.[23,30,31] When a solid sample of $[K(18\text{-c-}6)_2][Tb(NR_2)_3]$, **3-Tb**, prepared under argon, is dissolved in a nitrogen-containing glovebox in 35 °C Et_2O saturated with dinitrogen, the color changes gradually from

https://dx.doi.org/10.1021/jacs.0c01021
J Am Chem Soc 2020 142 9302 9313

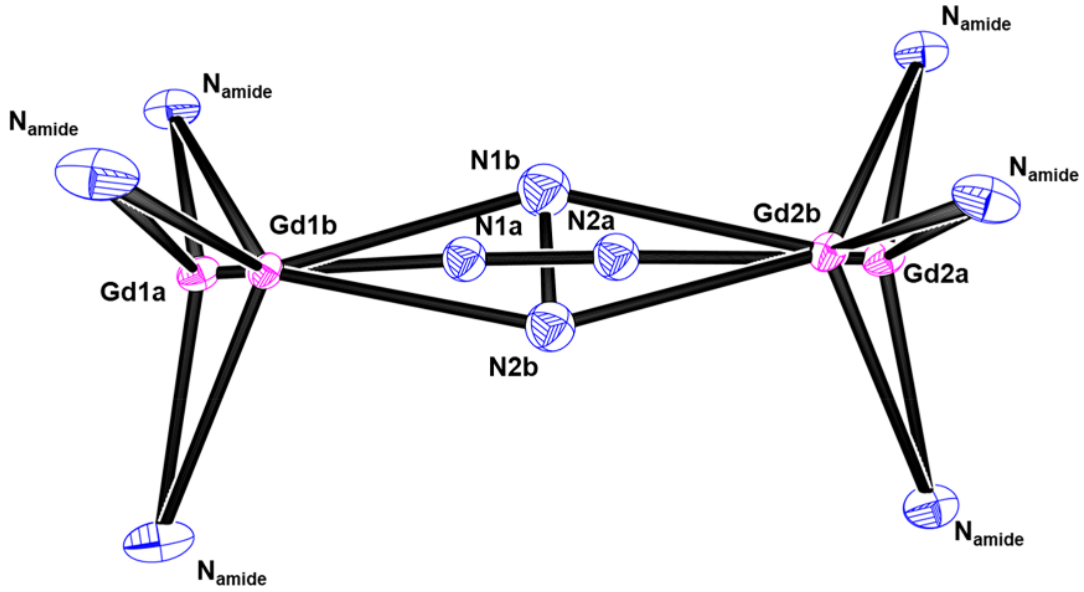

Figure 4. ORTEP representation of the disordered core of $[K_2(18\text{-c-}6)_3]\{[(R_2N)_3Gd]_2[\ -\eta^x{:}\eta^x\text{-}N_2]\}$ (x = 1, 2), **6-Gd**, drawn at the 50 probability level. Hydrogen atoms, counter-cations, $SiMe_3$ groups, and Et_2O molecules were excluded for clarity.

dark blue to pale yellow. Crystallization by ltration into a cold vial and replacement in the glovebox freezer produces the end-on complex, $[K_2(18\text{-c-}6)_3]\{[(R_2N)_3Tb]_2[\ -\eta^1{:}\eta^1\text{-}N_2]\}$, **4-Tb**. Unfortunately, crystals of this complex were not of sufficient quality for detailed metrical analysis.

The Raman spectra of **2-Tb** and **4-Tb** were nearly indistinguishable and displayed signals at 1630 and 1623 cm ^{1}, respectively, Figure 5. This is in the range of the Raman shift observed for the N_2 unit in **2-Sc**[21] at 1644 cm ^{1} and distinct from the more common side-on complexes, $[(THF)(R_2N)_2Ln]_2[\ -\eta^2{:}\eta^2\text{-}N_2]$, **7-Ln**, known for Ln = Nd, Gd, Tb, Dy, Ho, Y, Er, and Tm, which show Raman shift values ranging from 1417 to 1447 cm ^{1}.[28] The difference in these Raman shifts is consistent with the N N distance which is shorter in the dianionic end-on complex, **2-Tb**, than in the neutral side-on complexes, **7-Ln**. The 1623 1630 cm ^{1} stretching frequencies are in line with a moderately activated N_2 unit and fall in between those for free N_2, 2230 cm ^{1}, and N_2H_2, 1583 and 1529 cm ^{1}.[32 34]

Mixed End-on Side-on Complexes. The gadolinium complex, $[K(crypt)][Gd(NR_2)_3]$, **1-Gd**, reacted similarly but gave a different result from that obtained for **1-Tb** in eq 4. When **1-Gd**, prepared under Ar, is dissolved in N_2-saturated Et_2O at 35 °C, the solution turns gradually to a pale-yellow color after 5 min. Crystallization at 35 °C yields crystals with the same composition as **2-Tb**, but the product contains both side-on and end-on reduced dinitrogen ligands disordered over the two binding modes: $[K(crypt)]_2\{[(R_2N)_3Gd]_2[\ -\eta^x{:}\eta^x\text{-}N_2]\}[$ (x = 1 and 2), **5-Gd**, Figure 3.

The crystal data were modeled best with 70 side-on and 30 end-on occupancy, respectively. This is the rst example of a lanthanide complex of a side-on (N N)^2 ligand with three ancillary amide ligands on each lanthanide (cf. eq 2). The Gd center is also disordered in the structure with the same occupancies as the corresponding (N N)^2 binding modes.

Interestingly, the mixed binding mode complex **5-Gd** is isomorphous with the pure end-on scandium complex, $[K(crypt)]_2\{[(R_2N)_3Sc]_2[\ -\eta^1{:}\eta^1\text{-}N_2]\}$, **2-Sc**. In addition, these complexes crystallize in the same space group with comparable unit cell parameters as $[K(crypt)]_2\{[(R_2N)_3Gd]_2(\ -O)\}$, **10-Gd**, which was isolated and crystallographically characterized as part of this study (see Supporting Information). In one instance, **5-Gd** and **10-Gd** were observed to cocrystallize with 85 of the crystal modeled as **5-Gd end-on**) and the other 15 modeled as **10-Gd**. Unfortunately, neither the crystal of **10-Gd** nor the mixed crystal of **5**/**10-Gd** were of sufficient quality for metrical analysis.

The 18-c-6 Gd(II) complex, $[K(18\text{-c-}6)_2][Gd(NR_2)_3]$ **3-Gd**, also reacts with N_2 to form crystals containing both end-on and side-on (N N)^2 : $[K_2(18\text{-c-}6)_3]\{[(R_2N)_3Gd]_2[\ -\eta^x{:}\eta^x\text{-}N_2]\}$ (x = 1, 2), **6-Gd**. The core atoms of **6-Gd** are shown in Figure 4. The crystal data were modeled best with 50 side-on and 50 end-on occupancy. Complexes of **5-Gd** and **6-Gd** were isolated only as crystalline product with yields of 10 20 .

The disorder in **5-Gd** and **6-Gd** limits the conclusions that can be drawn from the structural data shown in Table 1. The end-on components of **5-Gd** and **6-Gd** are similar and differ from the side-on components of **5-Gd** and **6-Gd**, which are also similar. In the end-on structures, the metal is 0.40(4) 0.46(2) Å out of the plane of the three nitrogen donors of the three amide ligands. In the side-on components, the distances are 0.906(12) and 0.97(2) Å. In comparison, the pure end-on complexes, **2-Sc** and **2-Tb**, have out-of-plane distances between 0.678(3) and 0.663(1) Å, respectively.

The Ln N(N_2) distances of the end-on components in **5-Gd** and **6-Gd** are shorter than those of the side-on components, 2.155(9) Å for **5-Gd end-on**) vs 2.363(6) Å for **5-Gd side-on**) and 2.181(2) Å **6-Gd end-on**) vs 2.367(9) Å for **6-Gd side-on**). The Ln N(NR_2) distances span a wide range in **5-Gd** and **6-Gd**, 2.216(2) 2.486(2) Å, but in general the end-on structures have shorter Ln N(NR_2) distances (2.216(2) 2.295(2) Å, **5-Gd**; 2.286(3) 2.326(3)Å, **6-Gd**) than the side-on structures (2.371(2) 2.444(2) Å, **5-Gd**; 2.418(3) 2.486(3) Å, **6-Gd**). Hence, the Ln(N_3 plane), Ln N(N_2), and Ln N(NR_2) distances all are consistent with a more crowded coordination environment for the side-on complexes versus the end-on complexes.

https://dx.doi.org/10.1021/jacs.0c01021
J Am Chem Soc 2020 142 9302 9313

Table 1. Selected Bond Distances Å) of [K crypt)]$_2${[$R_2N)_3Sc]_2$[-η^1:η^1-N_2]}, 2-Sc,[21] [K crypt)]$_2${[$R_2N)_3Tb]_2$[-η^1:η^1-N_2]}, 2-Tb, [K crypt)]$_2${[$R_2N)_3Gd]_2$[-η :η -N_2]}[= 1 and 2), 5-Gd, and [K_2 18-c-6)$_3$]{[$R_2N)_3Gd]_2$[-η :η -N_2]} = 1, 2), 6-Gd

	Ln N(NR_2)$_{avg}$ [range]	Ln N(N_2)$_{avg}$	Ln (N_3 plane)$_{avg}$[a]	N N(N_2)
2-Sc	2.150(6) [2.143(2) 2.161(2)]	2.031(1)	0.678(3)	1.221(3)
2-Tb	2.326(6) [2.3126(19) 2.3406(19)]	2.189(2)	0.663(1)	1.217(3)
5-Gd end-on)	2.268(27) [2.216(2) 2.295(2)]	2.155(9)	0.40(4)	1.271(12)
5-Gd side-on)	2.408(26) [2.371(2) 2.444(2)]	2.363(3)	0.906(12)	1.190(5)
6-Gd end-on)	2.302(16) [2.286(3) 2.326(3)]	2.181(2)	0.46(2)	1.234(9)
6-Gd side-on)	2.45(3) [2.418(3) 2.486(3)]	2.367(9)	0.97(2)	1.193(9)

[a]The distance of the Ln to the plane of the three nitrogen donor atoms of the three amide ligands.

It would normally be expected that the distances in **2-Tb** would be slightly shorter than those in **5-Gd** because the ionic radius of Tb is 0.013 Å smaller than that of Gd. However, the 2.189(2) Å Ln N(N_2) distance in **2-Tb** is numerically larger and equivalent within the 3σ uncertainty interval to the 2.155(9) Å distance in **5-Gd end-on**). The 2.3126(19) 2.3406(19) Å range of Ln N(NR_2) distances in **2-Tb** is on average longer than the 2.216(2) 2.295(2) Å Ln N(NR_2) distance range in **5-Gd end-on**). The fact that the distances in **2-Tb** are not shorter as expected from the ionic radii suggests there may be more steric crowding in the Tb complex. It is also possible that the disorder in the Gd complex leads to this difference in distances.

The Raman spectra of **5-Gd** and **6-Gd** show intense signals at 1634 and 1627 cm ^{1} similar to the 1630 cm ^{1} shift of the pure end-on complexes, **2-Sc**,[21] **2-Tb**, and **4-Tb**, Figure 5. This is surprising because modeling the crystallographic data shows more side-on than end-on in the solid state. However, the density functional theory (DFT) calculations (see below) show that the end-on N N stretching vibration is approximately 2 orders of magnitude more intense than that of the side-on complex. The 1450 1500 cm ^{1} region does not show the strong well-resolved signals typically observed for side-on complexes and requires further investigation.

Reversibility of N_2 Binding with Gd II). If a solution of **5-Gd** or **6-Gd** at 78 °C is warmed to room temperature, a color change from pale yellow to dark blue is observed. UV visible spectra of the dark blue color shows a broad, intense absorbance around 600 nm consistent with [Gd(NR_2)$_3$]^1 .[24] Upon cooling the solution back to 78 °C, the color reverts from deep blue back to pale yellow. The same phenomena are observed with **2-Tb** and **4-Tb**, eq 5. This is as expected entropically and was recently observed with the Ti(III) amide, {Ti^{III}[N-($CH_2CH_2NSiMe_3$)$_3$]}.[32]

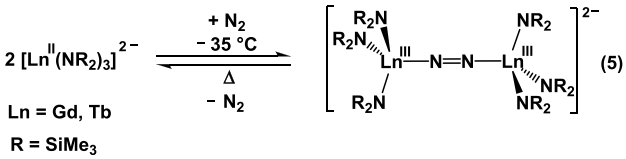

Isolation of a Side-on Bimetallic Complex with Five Amide Ancillary Ligands. When a solution of Gd(NR_2)$_3$ in THF cooled to 35 °C is added to a vial containing KC_8 cooled to 196 °C under N_2, yet a different type of reduced dinitrogen complex is observed. At this lower temperature, a side-on (N N)^2 complex is isolated in low yield where one Gd center is ligated by three amides and the other is ligated by two amides and a THF, i.e. [K(THF)$_6$]{[(THF)(R_2N)$_2$Gd][-η^2:η^2-N_2]-[Gd(NR_2)$_3$]}, **8-Gd**, eq 6, Figure 6. Additionally, crystals of [K(THF)$_6$][Gd(NR_2)$_4$], **11-Gd**, were isolated from the same reaction mixture (Supporting Information).

The structure of **8-Gd** is a monoanionic blend between the side-on neutral complex, [(THF)(R_2N)$_2$Gd]$_2$[-η^2:η^2-N_2]}, **7-Gd**,[9] with two amides and one THF per metal center, and the side-on components of **5-Gd** and **6-Gd**, which contain

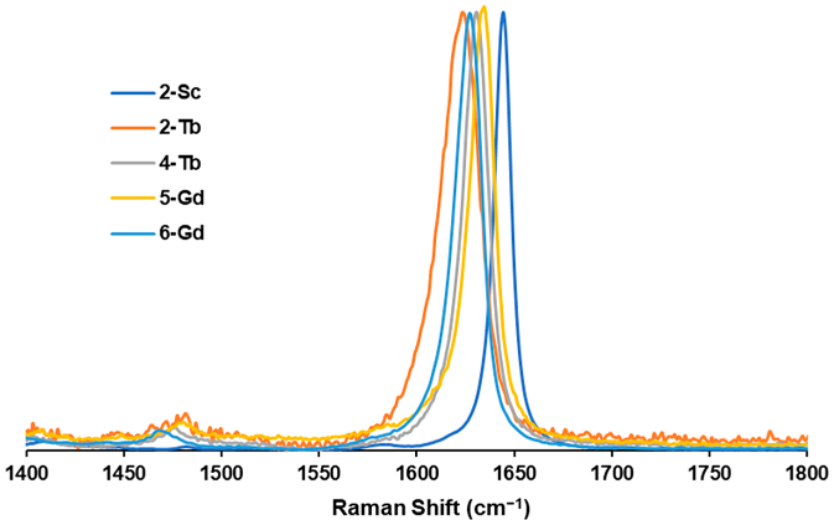

Figure 5. Normalized and baseline-corrected Raman spectra of **2-Sc** (1644 cm ^{1}),[21] **2-Tb** (1623 cm ^{1}), **4-Tb** (1630 cm ^{1}), **5-Gd** (1634 cm ^{1}), and **6-Gd** (1627 cm ^{1}). Individual spectra are shown in the Supporting Information.

https://dx.doi.org/10.1021/jacs.0c01021
J Am Chem Soc 2020 142 9302 9313

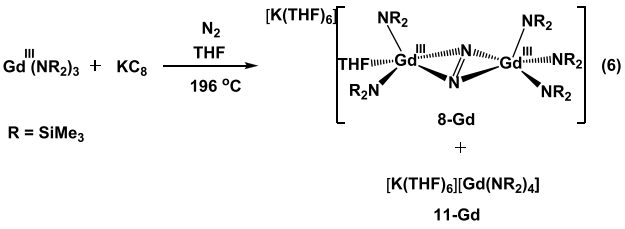

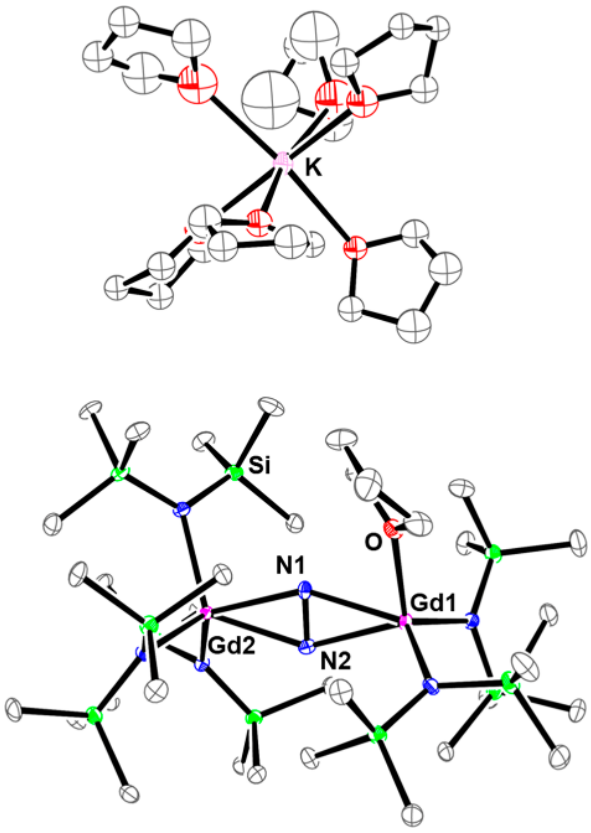

Figure 6. ORTEP representation of **8-Gd** drawn at the 50 probability level. Hydrogen atoms excluded for clarity (O = red, N = blue, Si = green, C = gray).

$\{[(R_2N)_3Gd]_2[\ -\eta^x{:}\eta^x\text{-}N_2]\}^2$ dianions and three amides per metal center. Metrical data are compared in Table 2. The 1.248(8) Å N N distance in side-on **8-Gd** is numerically intermediate between the 1.278(4) Å N N distance of side-on **7-Gd**, which has two amides per metal, and the 1.190(5) Å N N distance in **5-Gd side-on**), which has three amides per metal. However, the N N distance in **8-Gd** is equivalent within the 3σ uncertainty interval to that in **7-Gd** and as mentioned above, N N distances can vary from crystal to crystal.[28] The placement of the $(N\ \ N)^2$ ligand between the two types of Gd ions in **Gd-8** is not symmetrical. The 2.306(7) and 2.308(6) Å Gd(1) $N(N_2)$ distances for the metal with two amide ligands and one THF ligand [Gd(1)] are signi cantly shorter than the 2.449(6) and 2.399(6) Å Gd(2) $N(N_2)$ distances of the metal with three amide ligands [Gd(2)]. The two 2.310(6) and 2.313(6) Å Gd(1) $N(NR_2)$ distances are closer to the 2.333(6), 2.357(6), and 2.362(6) Å Gd(2) $N(NR_2)$ lengths. In general, the Gd(1) lengths are more similar to those in **3-Gd**, and the Gd(2) distances are more similar to those in **5-Gd side-on**), which is consistent with the coordination environments. The pyramidalization of the Gd(2) ion ligated by three amide ligands from the N_3 plane in **8-Gd**, 0.656 Å, is signi cantly less than that observed in **5-Gd side-on**), 0.902 Å. Conversely, the Gd(1) distance to the donor atom plane for the Gd ion containing two amide ligands and a THF in **8-Gd** is 0.833 Å, substantially larger than the 0.611 Å distance observed in **7-Gd**. These numbers are consistent with more steric crowding around Gd(1) which is closer to the $(N\ \ N)^2$ unit.

Formation of an $(N_2)^3$ Complex from Gd II). If a solid sample of **1-Gd** prepared under argon in 35 °C is dissolved in THF instead of Et_2O in a nitrogen- lled glovebox, an orange solution forms immediately. When the solution was ltered and layered with hexanes at 35 °C, crystals of the $(N_2)^3$ complex $[K(2.2.2\text{-crypt})]\{[(THF)(R_2N)_2Gd]_2[\ -\eta^2{:}\eta^2\text{-}N_2]\}$, **9-Gd**, were isolated in low yield, eq 7, Figure 7.

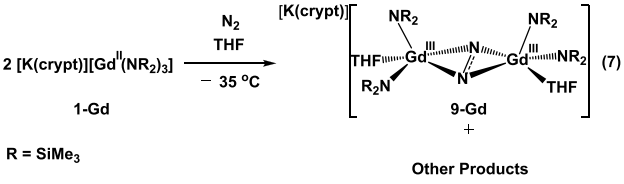

The structural data on **9-Gd** were not of sufficient quality for a detailed metrical analysis and comparison with other $(N_2)^3$ complexes,[19,35 38] but this result shows that Gd(II) is sufficiently reducing to convert $(N_2)^2$ to $(N_2)^3$. This is consistent with earlier results that showed that $(N_2)^3$ could be generated from divalent lanthanide ions, speci cally with Dy(II),[19] without the use of an alkali reducing agent.

Table 2. Selected Bond Distances Å) of $[K\ THF)_6]\{[\ THF)\ R_2N)_2Gd][\ -\eta^2{:}\eta^2\text{-}N_2][Gd\ NR_2)_3]\}$, 8-Gd, Compared to $[\ THF)\ R_2N)_2Gd]_2[\ -\eta^2{:}\eta^2\text{-}N_2]$, 7-Gd,[9] and the Side-on Component of 5-Gd, i.e. $[K\ crypt)]_2\{[\ R_2N)_3Gd]_2[\ -\eta^2{:}\eta^2\text{-}N_2]\}$

	Ln(1) N(1)(N_2)	Ln(1) N(2)(N_2)	Ln(1) N(1)(N_{NR2})	Ln(1) N(2)(N_{NR2})	Ln(1) O(1)(THF)/Ln(1) N(3)(N_{NR2})
7-Gd	2.326(2)	2.353(2)	2.2782(19)	2.2964(19)	2.4408(17)
5-Gd side-on)	2.361(4)	2.363(4)	2.415(2)	2.434(2)	2.381(2)
8-Gd	2.306(7)	2.308(6)	2.310(6)	2.313(6)	2.460(6)
	Ln(2) N(1)(N_2)	Ln(2) N(2)(N_2)	Ln(2) N(1)(N_{NR2})	Ln(2) N(2)(N_{NR2})	Ln(2) N(3)(N_{NR2})
7-Gd	2.326(2)				
5-Gd side-on)	2.369(4)	2.360(4)	2.371(2)	2.406(2)	2.444(2)
8-Gd	2.429(6)	2.399(6)	2.333(6)	2.357(6)	2.362(6)
	N(1) N(2)	Ln N_3(plane)	Ln NNO(plane)		
7-Gd	1.278(4)		0.611		
5-Gd side-on)	1.190(5)	0.902			
8-Gd	1.248(8)	0.656	0.833		

https://dx.doi.org/10.1021/jacs.0c01021
J Am Chem Soc 2020 142 9302 9313

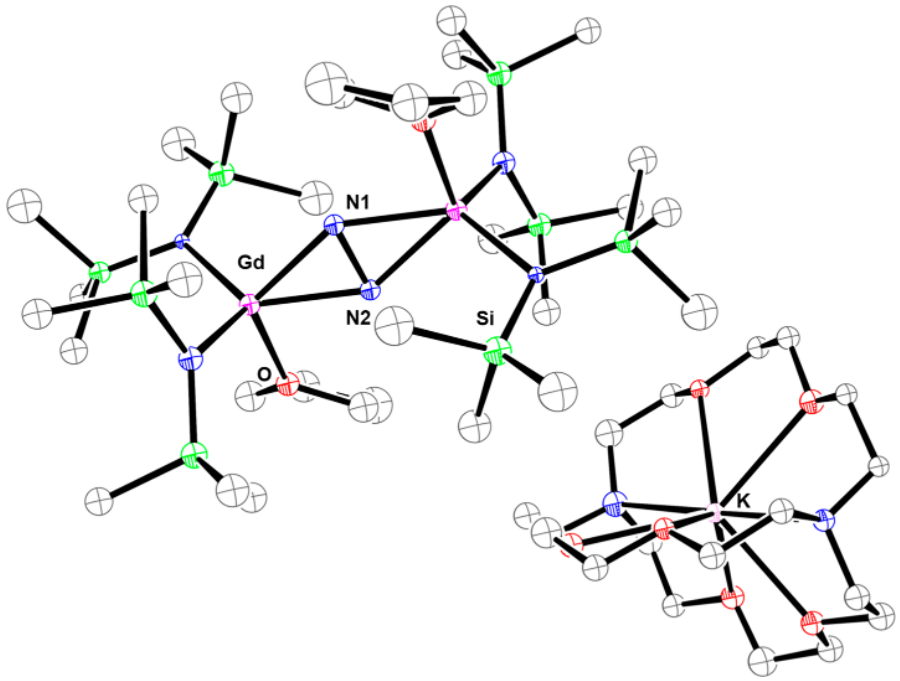

Figure 7. Ball and stick representation of **9-Gd**. Hydrogen atoms omitted for clarity (O = red, N = blue, Si = green, C = gray).

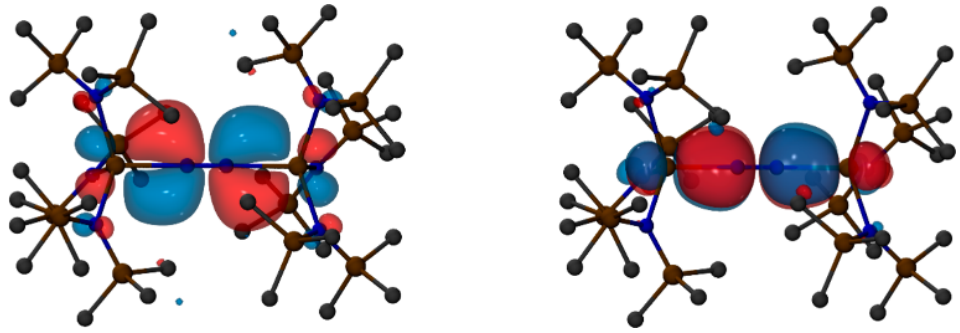

Figure 8. Degenerate HOMOs of $\{[(R_2N)_3Gd]_2[\ -\eta^1{:}\eta^1\text{-}N_2]\}^2$.

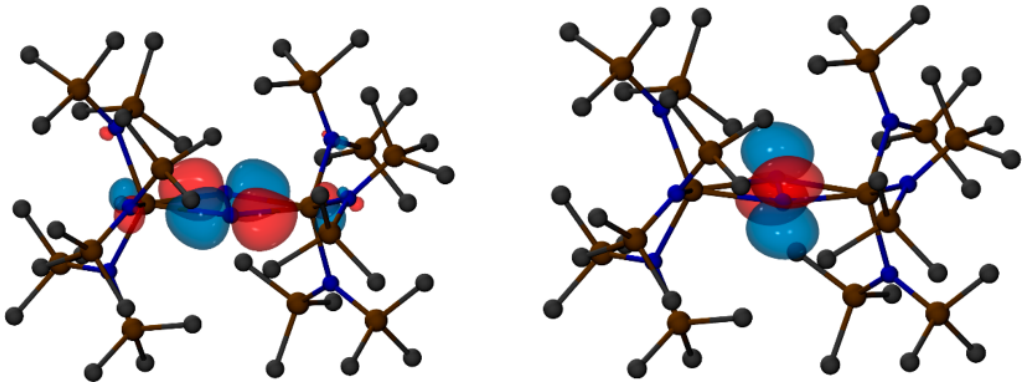

Figure 9. HOMO (left) and LUMO (right) of $\{[(R_2N)_3Gd]_2[\ -\eta^2{:}\eta^2\text{-}N_2]\}^2$.

Density Functional Calculations. The structures of the $\{[(R_2N)_3Gd]_2[\ -\eta^1{:}\eta^1\text{-}N\}^2$ (end-on) and $\{[(R_2N)_3Gd]_2[\ -\eta^2{:}\eta^2\text{-}N_2]\}^2$ (side-on) complexes were optimized using the TPSSh hybrid meta-generalized gradient approximation density functional and f-in-core effective core potentials (see Supporting Information for details). Optimization of the end-on complex resulted in a D_3-symmetric triplet ground state, while optimization of the side-on complex resulted in a C_2-symmetric singlet ground state.

The doubly degenerate HOMOs of the end-on complex exhibit metal-to-ligand δ-bonding character due to interactions of the antibonding π orbitals of the N_2 unit with the d_{xz} and d_{yz}

https://dx.doi.org/10.1021/jacs.0c01021
J Am Chem Soc 2020 142 9302 9313

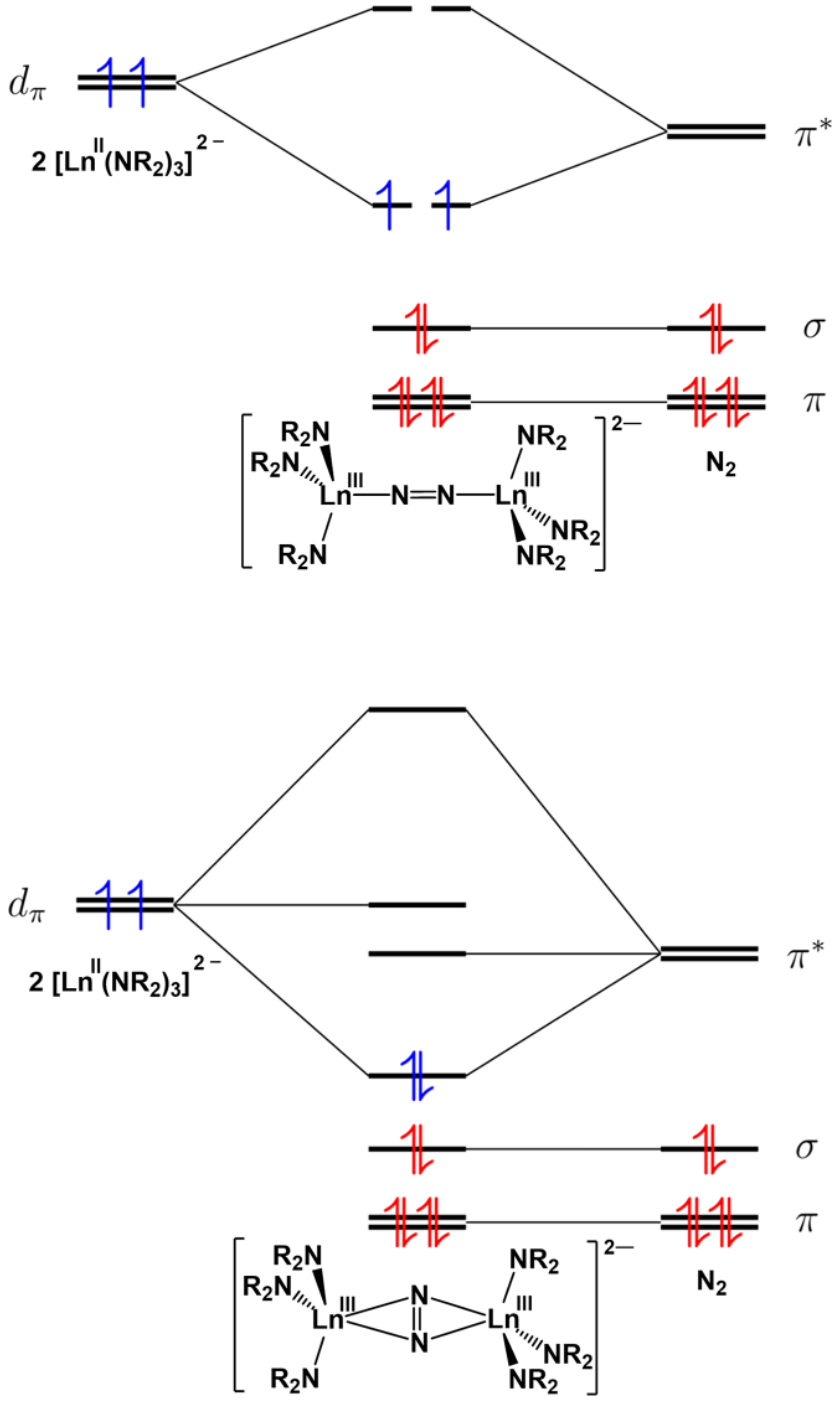

Figure 10. Qualitative MO representation of $\{[(R_2N)_3Gd]_2[\ -\eta^1{:}\eta^1\text{-}N_2]\}^2$ (top) and $\{[(R_2N_{)3}Gd]_2[\ -\eta^2{:}\eta^2\text{-}N_2]\}^2$ (bottom).

orbitals of the Gd atoms, Figure 8. In the side-on complex, on the other hand, only one of the two N_2 π orbitals can interfere constructively with the Gd d orbitals, producing a doubly occupied HOMO of metal-to-ligand π-bonding character, whereas the other N_2 π orbital remains unoccupied, Figure 9. A qualitative MO diagram showing the electronic structure of each complex is shown in Figure 10.

As in the case of the Sc compound,[21] end-on orientation of the N_2 unit leads to a degenerate HOMO favoring a triplet ground state, whereas side-on orientation lifts the degeneracy of the two N_2 π orbitals to such a degree that a singlet ground state is favorable. Based on the DFT calculations, the two structures are nearly isoenergetic within 2 kcal/mol, consistent with the isolation of both complexes under the same experimental conditions. The calculated geometrical details of the side-on and end-on complexes are given in the Supporting Information

The simulated vibrational Raman spectra suggest that the experimental spectrum in the 1500 1700 cm ^{1} region is dominated by the end-on complex, whose N N stretching vibration is approximately 2 orders of magnitude more intense than that of the side-on complex. The found ν_{NN} for the end-on

https://dx.doi.org/10.1021/jacs.0c01021
J Am Chem Soc 2020 142 9302 9313

anion in **5-Gd** and **6-Gd** was found to be 1663 cm ^{1}, which is close to the experimentally observed 1630 cm ^{1} value.

DISCUSSION

The reactions of solid Ln(II) tris(amide) complexes, [K-(crypt)][Ln(NR_2)$_3$], **1-Ln**, with N_2 to generate the reduced dinitrogen complexes, [K(crypt)]$_2${[(R_2N)$_3$Ln]$_2$[-η^x:η^x-N_2]}, (x = 1, **2-Tb**; x = 1, 2, **5-Gd**), constitute the rst hard evidence of Ln(II) intermediates in the previously known lanthanide amide reactions, Ln(NR_2)$_3$/K/N_2, that have formed [(THF)-(R_2N)$_2$Ln]$_2$[-η^2:η^2-N_2], **7-Ln**, complexes across the lanthanide series according to eq 2. Previously, it was unknown if the Ln(NR_2)$_3$/K/N_2 reactions involved Ln(II) intermediates,[9] because molecular species containing the La(II), Ce(II), Pr(II), Gd(II), Tb(II), Ho(II), Er(II), Lu(II), and Y(II) ions had not been discovered when the reduced dinitrogen complexes were isolated. Thus, the suggestion of Ln(II) intermediates in the formation of the **7-Ln** complexes was highly speculative before complexes of Ln(II) ions beyond the traditional Eu, Yb, Sm, Tm, Dy, and Nd examples were discovered.[31,39] Interestingly, the (N N)^2 products isolated from the reactions of isolated Ln(II) tris(amide) precursors are not the side-on **7-Ln**, complexes with two ancillary amide ligands per metal isolated from Ln(NR_2)$_3$/K/N_2 reactions, but the end-on {[(R_2N)$_3$Ln]$_2$[-η^1:η^1-N_2]}^{2} dianions with three amides per lanthanide.

Because these latter dianions have the same number of amides as the [Ln(NR_2)$_3$]^1 starting material, it is tempting to speculate that this is related to the mechanism of reduction. It is possible that the Ln(II) anion, [Ln(NR_2)$_3$]^1 , formed from Ln(NR_2)$_3$ and potassium, reduces N_2. Initial reduction could form an end-on {[(R_2N)$_3$Ln][N_2]}^{1} radical that is quickly trapped by another [Ln(NR_2)$_3$]^1 unit to form the end-on bimetallic complex, {[(R_2N)$_3$Ln]$_2$[-η^1:η^1-N_2]}^{2} , described for the rst time in this study. These complexes could thermally decompose to reform the Ln(II) precursors, [Ln(NR_2)$_3$]^1 , as observed here, or, if an (NR_2)^1 ligand is substituted by THF, a monoanionic complex of the type isolated in this study, {[(THF)(R_2N)$_2$Ln][-η^2:η^2-N_2][Ln(NR_2)$_3$]}^{1} , **8-Ln**, could form. A reviewer has pointed out that the substitution of an (NR_2)^1 ligand in {[(R_2N)$_3$Ln]$_2$[-η^1:η^1-N_2]}^{2} by THF would increase the electrophilicity of the Ln(III) ion, and this could lead to the end-on to side-on conversion. If an (NR_2)^1 ligand in **8-Ln** is displaced by THF, the nal product of the Ln(NR_2)$_3$/K/N_2 reactions results: [(THF)(R_2N)$_2$Ln]$_2$[-η^2:η^2-N_2], **7-Ln**. Because the earlier Ln(NR_2)$_3$/K/N_2 reactions were conducted at room temperature, the **1-Ln**, **2-Ln**, and **8-Ln** intermediates were not observed.

The fact that Gd(II) and Tb(II) complexes react with dinitrogen to form end-on bound (N N)^2 complexes, {[(R_2N)$_3$Ln]$_2$[-η^1:η^1-N_2]}^{2} , similar to those of Sc,[21] provides another example of the similarity of late Ln(II) chemistry with Sc(II) chemistry that is not shared by Y(II). Hence, the fact that [Y(NR_2)$_3$]^1 is much less stable than [Sc(NR_2)$_3$]^1 as well as the [Ln(NR_2)$_3$]^1 complexes of Ln = Gd, Tb, Dy, Ho, and Er is not an isolated example of nonanalogous Y(II) chemistry. Hence, it seems prudent to refrain from extending the similarity of Y(III) and the late lanthanide +3 ions to the +2 oxidation state. The origin of this effect is not clear, although nonperiodic chemistry is sometimes observed for 4d vs 3d and 5d transition metal complexes.[40,41]

The reversibility of eq 4 as the temperature is increased, i.e. eq 5, has parallels with the isolation of the rst lanthanide dinitrogen complex, [(C_5Me_5)$_2$Sm]$_2$[-η^2:η^2-N_2], eq 1. In that case, lower temperature favors the dinitrogen complex as expected based on entropy. This entropically driven binding of N_2 is also seen with the sterically crowded Ti amide complex {Ti^{III}[N($CH_2CH_2NSiMe_3$)$_3$]} which forms a bimetallic N_2 complex at low temperatures that breaks up upon warming.[32]

It is clear from this study and other related studies of lanthanide amide reduction reactions,[23,24] that the details of the speci c reactions are critical to the outcome. The isolation of the gadolinium crystals with mixed end-on and side-on ligation of N_2 is consistent with the DFT calculations which show the side-on and end-on structures to be nearly isoenergetic. This is in contrast to calculations performed on the end-on Sc complex which showed a hypothetical side-on bound structure to be 12 kcal/mol higher in energy than the end-on counterpart.[21] It is possible that by moving from Gd to its neighbor, Tb, which differs by being 0.013 Å smaller,[42] the balance between end-on and side-on shifts to favor the sterically less crowded end-on structure. This may be why **2-Tb** and **4-Tb** are purely end-on. Hence, selection of one lanthanide versus its adjacent element can influence the reaction.

Subtle differences in binding modes based on metal ion size and the steric pro le of the ligands have previously been observed in Ti and Zr dinitrogen chemistry. Reduction of the pentamethylcyclopentadienyl zirconium dichloride, (C_5Me_5)$_2$$ZrCl_2$, under a nitrogen atmosphere will reductively bind dinitrogen and form a bimetallic end-on bound N_2 complex, [(C_5Me_5)$_2$(N_2)Zr]$_2$(-η^1:η^1-N_2).[43,44] In contrast, when the *tetra*-methylcyclopentadienyl zirconium dichloride complex, (C_5Me_4H)$_2$$ZrCl_2$, is reduced under dinitrogen, the side-on bound dinitrogen complex [(C_5Me_4H)$_2$Zr]$_2$(-η^2:η^2-N_2), is observed.[45,46] In the case of smaller titanium, however, both C_5Me_5 and C_5Me_4H ligands are large enough to give end-on bound dinitrogen complexes [(C_5Me_4R)$_2$Ti]$_2$(-η^1:η^1-N_2) (R = H, Me),[47,48] and a trimethylcyclopentadienyl ligand is needed to observe the side-on binding mode, [($C_5Me_3H_2$)$_2$Ti]$_2$(-η^2:η^2-N_2).[49,50]

Temperature is also crucial: under the conditions of the previously reported Ln(NR_2)$_3$/K/N_2 reactions, [(THF)-(R_2N)$_2$Ln]$_2$[-η^2:η^2-N_2], **7-Ln**, would be the only isolated product. To observe the Ln(II) and Ln N N Ln intermediates, low temperatures and fast reaction times are necessary. This study also showed that conducting these reactions in THF vs Et_2O can lead to an (N_2)^3 product rather than (N N)^2 products. This result also shows that Gd(II) is capable of forming (N_2)^3 because no alkali metal was present in the formation of **9-Gd**.

The structural similarity of the end-on (N N)^2 , side-on (N N)^2 , and O^2 complexes suggests that other small dianions should t inside two [Ln(NR_2)$_3$]^1 units. Long ago, Lappert reported a [(R_2N)$_3$Ce]$_2$[-η^2:η^2-O_2] complex showing this structural motif with (O_2)^2 and Ce(IV).[51] It remains to be determined if such species are best accessed through [Ln-(NR_2)$_3$]^1 , {[(R_2N)$_3$Ln]$_2$[-η^x:η^x-N_2]}^{2} , or some other precursor. In any case, the success of such a reaction is likely to involve the speci c countercation as these have been found to be crucial to isolate (and crystallize) speci c samples of reduced complexes.[23,24,52]

CONCLUSION

For over 30 years, crystallographic analysis of lanthanide-based dinitrogen reduction products has provided structures of only side-on Ln_2N_2 complexes, i.e. [(solvent)A_2Ln]$_2$[-η^2:η^2-N_2]

https://dx.doi.org/10.1021/jacs.0c01021
J Am Chem Soc 2020 142 9302 9313

with A = anion. The mechanism of the $LnA_3/K/N_2$ reactions that formed these complexes was unknown. Now, the rst examples of end-on lanthanide Ln N N Ln species have been isolated, $[K(crypt)]_2\{[(R_2N)_3Ln]_2[\ -\eta^1{:}\eta^1\text{-}N_2]\}$. The end-on structures were obtained by using the isolated Ln(II) complexes, $[K(chelate)][Ln(NR_2)_3]$, as the reductant instead of the in situ product generated from $Ln(NR_2)_3$ and K and by doing the reactions at low temperature. This shows the Ln(II) complexes can indeed be involved in these reactions. The fact that warming the Gd(III) (N N)^2 complex to room temperature reforms the Gd(II) precursor indicates that the Gd(III)/Gd(II) and $N_2/(N_2)^2$ reduction potentials are closely matched. The isolation of the penta-amide complex, $[K(THF)_6]\{[(THF)(R_2N)_2Gd][\ -\eta^2{:}\eta^2\text{-}N_2][Gd(NR_2)_3]\}$, suggests that lanthanide-based reduction of N_2 can occur by reaction of 2 equiv of the divalent $[Ln(NR_2)_3]^1$ with N_2 to form an end-on dianion, $\{[(R_2N)_3Ln]_2[\ -\eta^1{:}\eta^1\text{-}N_2]\}^2$, which can lose one $(NR_2)^1$ ligand per metal to form the neutral side-on $[(THF)(R_2N)_2Ln]_2[\ -\eta^2{:}\eta^2\text{-}N_2]$ complex. The speci c product isolated in these lanthanide-based dinitrogen reduction reactions depends critically on the details of the experimental conditions including temperature, solvent, reaction time, and the presence or absence of a chelate. This study also provided more evidence to suggest that Sc(II) and the late lanthanide Ln(II) ions are similar and differ from Y(II). Hence, Y(III) is similar to the late trivalent lanthanides and has congeneric similarities to Sc(III); yttrium in the +2 oxidation state should be considered neither a surrogate for the late lanthanides nor a congeneric analogue of Sc(II).

EXPERIMENTAL DETAILS

All manipulations and syntheses described below were conducted with the rigorous exclusion of air and water using standard Schlenk line and glovebox techniques under an argon or dinitrogen atmosphere. Solvents were sparged with UHP argon and dried by passage through columns containing Q-5 and molecular sieves prior to use. Elemental analyses were conducted on a PerkinElmer 2400 Series II CHNS elemental analyzer. Complexes of **1-Ln**[24] and **3-Ln**[23] were synthesized as previously reported. Infrared spectra were collected on an Agilent Cary 630 equipped with a diamond ATR attachment. Raman spectra were collected on solid samples in a 1 mm quartz cuvette appended with a Teflon stopcock using a Renishaw inVia confocal Raman Microscope, equipped with a 122 mW laser of wavelength 785 nm (laser power 10 and a X5L objective laser). Measurements were taken on at least three different crystals to con rm reproducibility while one of the spectra is reported.

[K crypt)]$_2$[[$R_2N)_3Tb]_2[\ -\eta^1{:}\eta^1$-$N_2]$], 2-Tb. In a dinitrogen lled glovebox, $[K(crypt)][Tb(NR_2)_3]$ (40 mg, 0.038 mmol), **1 Tb**, was dissolved in 35 °C, nitrogen saturated, Et_2O and placed in the freezer overnight. The resulting yellow solution produced crystals suitable for X-ray diffraction (9 mg, 11 yield). IR: 2942s, 2889s, 2817m, 2762w, 2730w, 2698w, 1478m, 1458m, 1446m, 1356s, 1299m, 1260s 1237s, 1135s, 1107s, 1078s, 1059s, 992s, 952s, 933m, 869s, 827s, 770m, 752m, 713m, 691m, 663s, cm ^{1}. Anal. Calcd for $C_{72}H_{180}N_{12}O_{12}Si_{12}K_2Tb_2$: C, 40.42; H, 8.48; N, 7.86. Found: C, 39.95; H, 8.04; N, 7.23.

[K_2 18-c-6)$_3$]{[$R_2N)_3Tb]_2[\ -\eta^1{:}\eta^1$-$N_2]$}, 4-Tb. In a dinitrogen lled glovebox, $[K(18c6)_2][Tb(NR_2)_3]$ (40 mg, 0.038 mmol) was dissolved in 35 °C, nitrogen saturated, Et_2O and placed in the freezer overnight. The resulting yellow solution produced crystals suitable for X-ray diffraction (13 mg, 17). IR: 2938m, 2887m, 1472w, 1453w, 1352m, 1237s, 1104s, 945s, 865m, 813s, 771m, 700m, 653s cm ^{1}. Anal. Calcd for $C_{72}H_{180}N_8O_{18}Si_{12}K_2Tb_2$: C, 39.68; H, 8.33; N, 5.15. Found: C, 39.25; H, 8.71; N, 5.50.

[K crypt)]$_2${[$R_2N)_3Gd]_2[\ -\eta\ :\eta\ -N_2]$} = 1, 2), 5-Gd. In a nitrogen lled glovebox, $[K(crypt)][Gd(NR_2)_3]$ (40 mg, 0.037 mmol) was dissolved in 35 °C, nitrogen saturated, Et_2O and placed in the freezer overnight. The resulting yellow solution produced crystals suitable for X-ray diffraction (7 mg, 9). IR: 2942s, 2890s, 2819m, 2762w, 2729w, 2697w, 1478m, 1459m, 1446m, 1356s, 1298m, 1260s 1236s, 1135s, 1107s, 1078s, 1060s, 996s, 952s, 934m, 869s, 825s, 769m, 751m, 711m, 690m, 662s, cm ^{1}. Anal. Calcd for $C_{72}H_{180}N_{12}O_{12}Si_{12}K_2Gd_2$: C, 40.49; H, 8.49; N, 7.87. Found: C, 39.35; H, 8.91; N, 7.61.

[K_2 18-c-6)$_3$]{[$NR_2)_3Gd]_2[\ -\eta\ :\eta\ -N_2]$} X = 1, 2), 6-Gd. In a dinitrogen lled glovebox, $[K(18c6)_2][Gd(NR_2)_3]$ (40 mg, 0.033 mmol) was dissolved in 35 °C, nitrogen saturated, Et_2O and placed in the freezer overnight. The resulting yellow solution produced crystals suitable for X-ray diffraction (15 mg, 20 yield). Anal. Calcd for $C_{72}H_{180}N_{12}O_{12}Si_{12}K_2Gd_2$: C, 39.74; H, 8.34; N, 5.15. Found: C, 39.25; H, 8.90; N, 4.56.

[K THF)$_6$]{[THF) $R_2N)_2Gd][\ -\eta^2{:}\eta^2$-$N_2$][Gd $NR_2)_3$]}, 8-Gd, and [K THF)$_6$][Gd $NR_2)_4$] 11-Gd. In a dinitrogen lled glovebox, Gd-$(NR_2)_3$ was dissolved in 35 °C, nitrogen saturated, THF and then added to a vial containing KC_8 at 77 K. The solution was immediately ltered and layered with 35 °C hexanes and replaced in the glovebox freezer. The resulting orange solution produced crystals of **8-Gd** and **11-Gd** suitable for X-ray diffraction after 24 h.

[K crypt)]{ THF)[$R_2N)_2Gd]_2[\ -\eta^2{:}\eta^2$-$N_2]$}, 9-Gd. In a dinitrogen lled glovebox, $[K(crypt)][Gd(NR_2)_3]$ was dissolved in 35 °C, nitrogen saturated, THF and placed in the freezer overnight. The resulting orange solution produced crystals of **9-Gd** suitable for X-ray diffraction.

X-ray Crystallographic Data. Crystallographic information for complexes **2-Tb**, **3-Tb**, **4-Tb**, **5-Gd**, **6-Gd**, **8-Gd**, **9-Gd**, **10-Gd**, and **11-Gd**, is summarized in the Supporting Information.

ASSOCIATED CONTENT

Supporting Information

The Supporting Information is available free of charge at https://pubs.acs.org/doi/10.1021/jacs.0c01021.

Crystallographic details for **2-Tb**, **4-Tb**, **5-Gd**, **6-Gd**, **8-Gd**, **9-Gd**, **10-Gd**, and **11-Gd** (PDF)

Crystallographic information le (**2-Tb**) (CIF)

Crystallographic information le (**6-Gd**) (CIF)

Crystallographic information le (**5-Gd**) (CIF)

Crystallographic information le (**8-Gd**) (CIF)

Crystallographic information le (**11-Gd**) (CIF)

AUTHOR INFORMATION

Corresponding Authors

William J Evans *Department of Chemistry University of California Irvine California 92697-2025 United States;* orcid.org/0000-0002-0651-418X; Email: wevans@uci.edu

Filipp Furche *Department of Chemistry University of California Irvine California 92697-2025 United States;* orcid.org/0000-0001-8520-3971; Email: lipp.furche@uci.edu

Authors

Austin J Ryan *Department of Chemistry University of California Irvine California 92697-2025 United States;* orcid.org/0000-0003-0983-0150

Sree ganesh Balasubramani *Department of Chemistry University of California Irvine California 92697-2025 United States*

Joseph W Ziller *Department of Chemistry University of California Irvine California 92697-2025 United States;* orcid.org/0000-0001-7404-950X

Complete contact information is available at: https://pubs.acs.org/10.1021/jacs.0c01021

Notes

The authors declare no competing nancial interest.

ACKNOWLEDGMENTS

The experimental part of this research was supported by the National Science Foundation under CHE-1855328 (W.J.E.), and theoretical studies were supported by CHE-1800431 (F.F.). We acknowledge Dmitry Fishman and the UCI Laser Spectroscopy Laboratories for assistance with Raman spectroscopy.

REFERENCES

(1) Evans, W. J.; Ulibarri, T. A.; Ziller, J. W. Isolation and X-ray crystal structure of the first dinitrogen complex of an f-element metal, $[(C_5Me_5)_2Sm]_2N_2$. *J. Am. Chem. Soc.* **1988**, *110* (20), 6877 6879.
(2) Tanabe, Y. Group 3 Transition Metal, Lanthanide, and Actinide-Dinitrogen Complexes. In *Transition Metal-Dinitrogen Complexes*; Nishibayashi, Y. Ed.; Wiley-VCH: 2019; pp 441 474.
(3) Evans, W. J.; Allen, N. T.; Ziller, J. W. Facile Dinitrogen Reduction via Organometallic Tm(II) Chemistry. *J. Am. Chem. Soc.* **2001**, *123* (32), 7927 7928.
(4) Evans, W. J.; Allen, N. T.; Ziller, J. W. Expanding Divalent Organolanthanide Chemistry: The First Organothulium(II) Complex and the In Situ Organodysprosium(II) Reduction of Dinitrogen. *Angew. Chem. Int. Ed.* **2002**, *41* (2), 359 361.
(5) Evans, W. J.; Kozimor, S. A.; Ziller, J. W. A Monometallic f Element Complex of Dinitrogen: $(C_5Me_5)_3U(\eta\text{-}N_2)$. *J. Am. Chem. Soc.* **2003**, *125* (47), 14264 14265.
(6) Evans, W. J.; Lee, D. S. Early developments in lanthanide-based dinitrogen reduction chemistry. *Can. J. Chem.* **2005**, *83* (4), 375 384.
(7) Evans, W. J.; Lee, D. S.; Johnston, M. A.; Ziller, J. W. The Elusive $(C_5Me_4H)_3Lu$: Its Synthesis and $LnZ_3/K/N_2$ Reactivity. *Organometallics* **2005**, *24* (26), 6393 6397.
(8) Evans, W. J.; Lee, D. S.; Lie, C.; Ziller, J. W. Expanding the LnZ_3/Alkali-Metal Reduction System to Organometallic and Heteroleptic Precursors: Formation of Dinitrogen Derivatives of Lanthanum. *Angew. Chem. Int. Ed.* **2004**, *43* (41), 5517 5519.
(9) Evans, W. J.; Lee, D. S.; Rego, D. B.; Perotti, J. M.; Kozimor, S. A.; Moore, E. K.; Ziller, J. W. Expanding Dinitrogen Reduction Chemistry to Trivalent Lanthanides via the LnZ_3/Alkali Metal Reduction System: Evaluation of the Generality of Forming $Ln_2(\ -\eta^2{:}\eta^2\text{-}N_2)$ Complexes via LnZ_3/K. *J. Am. Chem. Soc.* **2004**, *126* (44), 14574 14582.
(10) Evans, W. J.; Lee, D. S.; Ziller, J. W. Reduction of Dinitrogen to Planar Bimetallic $M_2(\ -\eta^2{:}\eta^2\text{-}N_2)$ Complexes of Y, Ho, Tm, and Lu Using the $K/Ln[N(SiMe_3)_2]_3$ Reduction System. *J. Am. Chem. Soc.* **2004**, *126* (2), 454 455.
(11) Evans, W. J.; Lee, D. S.; Ziller, J. W.; Kaltsoyannis, N. Trivalent $[(C_5Me_5)_2(THF)Ln]_2(\ -\eta^2{:}\eta^2\text{-}N_2)$ Complexes as Reducing Agents Including the Reductive Homologation of CO to a Ketene Carboxylate, $(\ -\eta^4\text{-}O_2CCCO)_2$. *J. Am. Chem. Soc.* **2006**, *128* (43), 14176 14184.
(12) Evans, W. J.; Zucchi, G.; Ziller, J. W. Dinitrogen Reduction by Tm(II), Dy(II), and Nd(II) with Simple Amide and Aryloxide Ligands. *J. Am. Chem. Soc.* **2003**, *125* (1), 10 11.
(13) Mansell, S. M.; Kaltsoyannis, N.; Arnold, P. L. Small Molecule Activation by Uranium Tris(aryloxides): Experimental and Computational Studies of Binding of N_2, Coupling of CO, and Deoxygenation Insertion of CO_2 under Ambient Conditions. *J. Am. Chem. Soc.* **2011**, *133* (23), 9036 9051.
(14) Campazzi, E.; Solari, E.; Floriani, C.; Scopelliti, R. The fixation and reduction of dinitrogen using lanthanides: praseodymium and neodymium meso-octaethylporphyrinogen dinitrogen complexes. *Chem. Commun.* **1998**, *23*, 2603 2604.
(15) Cheng, J.; Takats, J.; Ferguson, M. J.; McDonald, R. Heteroleptic Tm(II) Complexes: One More Success for Trofimenko s Scorpionates. *J. Am. Chem. Soc.* **2008**, *130* (5), 1544 1545.
(16) Cloke, F. G. N.; Hitchcock, P. B. Reversible Binding and Reduction of Dinitrogen by a Uranium(III) Pentalene Complex. *J. Am. Chem. Soc.* **2002**, *124* (32), 9352 9353.
(17) Roussel, P.; Scott, P. Complex of Dinitrogen with Trivalent Uranium. *J. Am. Chem. Soc.* **1998**, *120* (5), 1070 1071.
(18) Jaroschik, F.; Momin, A.; Nief, F.; Le Goff, X. F.; Deacon, G. B.; Junk, P. C. Dinitrogen Reduction and C-H Activation by the Divalent Organoneodymium Complex $[(C_5H_2{}^tBu_3)_2Nd(\ -I)K([18]\text{crown-}6)]$. *Angew. Chem.* **2009**, *121* (6), 1137 1141.
(19) Evans, W. J.; Fang, M.; Zucchi, G.; Furche, F.; Ziller, J. W.; Hoekstra, R. M.; Zink, J. I. Isolation of dysprosium and yttrium complexes of a three-electron reduction product in the activation of dinitrogen, the $(N_2)^3$ radical. *J. Am. Chem. Soc.* **2009**, *131* (31), 11195 11202.
(20) Evans, W. J.; Fang, M.; Bates, J. E.; Furche, F.; Ziller, J. W.; Kiesz, M. D.; Zink, J. I. Isolation of a radical dianion of nitrogen oxide $(NO)^2$. *Nat. Chem.* **2010**, *2* (8), 644.
(21) Woen, D. H.; Chen, G. P.; Ziller, J. W.; Boyle, T. J.; Furche, F.; Evans, W. J. End-on bridging dinitrogen complex of scandium. *J. Am. Chem. Soc.* **2017**, *139* (42), 14861 14864.
(22) Cleaves, P. A.; King, D. M.; Kefalidis, C. E.; Maron, L.; Tuna, F.; McInnes, E. J. L.; McMaster, J.; Lewis, W.; Blake, A. J.; Liddle, S. T. Two-Electron Reductive Carbonylation of Terminal Uranium(V) and Uranium(VI) Nitrides to Cyanate by Carbon Monoxide. *Angew. Chem. Int. Ed.* **2014**, *53* (39), 10412 10415.
(23) Ryan, A. J.; Ziller, J. W.; Evans, W. The Importance of the Counter-cation in Reductive Rare-Earth Metal Chemistry: Isolation of $[Y^{II}(NR_2)_3]^1$ and CO Reactivity to Form Ynediolate and Enediolate Complexes. *Chemical Science* **2020**, *11* (7), 2006 2014.
(24) Ryan, A. J.; Darago, L. E.; Balasubramani, S. G.; Chen, G. P.; Ziller, J. W.; Furche, F.; Long, J. R.; Evans, W. J. Synthesis, Structure, and Magnetism of Tris (amide) $[Ln\{N(SiMe_3)_2\}_3]^1$ Complexes of the Non-traditional + 2 Lanthanide Ions. *Chem. - Eur. J.* **2018**, *24* (30), 7702 7709.
(25) Corbey, J. F.; Woen, D. H.; Palumbo, C. T.; Fieser, M. E.; Ziller, J. W.; Furche, F.; Evans, W. J. Ligand Effects in the Synthesis of Ln2+ Complexes by Reduction of Tris(cyclopentadienyl) Precursors Including C H Bond Activation of an Indenyl Anion. *Organometallics* **2015**, *34* (15), 3909 3921.
(26) Moehring, S. A.; Beltran-Leiva, M. J.; Paez-Hernandez, D.; Arratia-Perez, R.; Ziller, J. W.; Evans, W. J. Rare-Earth Metal(II) Aryloxides: Structure, Synthesis, and EPR Spectroscopy of $[K(2.2.2\text{-cryptand})][Sc(OC6H_2{}^tBu_2\text{-}2,6\text{-Me-}4)_3]$. *Chem. - Eur. J.* **2018**, *24* (68), 18059 18067.
(27) Holland, P. L. Metal dioxygen and metal dinitrogen complexes: where are the electrons? *Dalt. Trans.* **2010**, *39* (23), 5415 5425.
(28) Fieser, M. E.; Woen, D. H.; Corbey, J. F.; Mueller, T. J.; Ziller, J. W.; Evans, W. J. Raman spectroscopy of the N N bond in rare earth dinitrogen complexes. *Dalt. Trans.* **2016**, *45* (37), 14634 14644.
(29) Hitchcock, P. B.; Hulkes, A. G.; Lappert, M. F.; Li, Z. Cerium(iii) dialkyl dithiocarbamates from $[Ce\{N(SiMe_3)_2\}_3]$ and tetraalkylthiuram disulfides, and $[Ce(\kappa^2\text{-}S_2CNEt_2)_4]$ from the CeIII precursor; TbIII and NdIII analogues. *Dalt. Trans.* **2004**, *1*, 129 136.
(30) MacDonald, M. R.; Ziller, J. W.; Evans, W. J. Synthesis of a Crystalline Molecular Complex of Y2+, [(18-crown-6)K]-[(C5H4SiMe3)3Y]. *J. Am. Chem. Soc.* **2011**, *133* (40), 15914 15917.
(31) MacDonald, M. R.; Bates, J. E.; Ziller, J. W.; Furche, F.; Evans, W. J. Completing the Series of + 2 Ions for the Lanthanide Elements: Synthesis of Molecular Complexes of Pr^{2+}, Gd^{2+}, Tb^{2+}, and Lu^{2+}. *J. Am. Chem. Soc.* **2013**, *135* (26), 9857 9868.
(32) Doyle, L. R.; Wooles, A. J.; Jenkins, L. C.; Tuna, F.; McInnes, E. J. L.; Liddle, S. T. Catalytic Dinitrogen Reduction to Ammonia at a Triamidoamine Titanium Complex. *Angew. Chem. Int. Ed.* **2018**, *57* (21), 6314 6318.
(33) Rasetti, F. On The Raman Effect in Diatomic Gases. *Proc. Natl. Acad. Sci. U. S. A.* **1929**, *15* (3), 234.
(34) Back, R. A.; Willis, C.; Ramsay, D. A. The Near-ultraviolet Absorption Spectrum of Diimide Vapor. *Can. J. Chem.* **1974**, *52* (6), 1006 1012.
(35) Meihaus, K. R.; Corbey, J. F.; Fang, M.; Ziller, J. W.; Long, J. R.; Evans, W. J. Influence of an Inner-Sphere K^+ Ion on the Magnetic

https://dx.doi.org/10.1021/jacs.0c01021
J Am Chem Soc 2020 142 9302 9313

Behavior of N_2^{3-} Radical-Bridged Dilanthanide Complexes Isolated Using an External Magnetic Field. *Inorg. Chem.* **2014**, *53* (6), 3099 3107.
(36) Fang, M.; Bates, J. E.; Lorenz, S. E.; Lee, D. S.; Rego, D. B.; Ziller, J. W.; Furche, F.; Evans, W. J. $(N_2)^{3-}$ Radical Chemistry via Trivalent Lanthanide Salt/Alkali Metal Reduction of Dinitrogen: New Syntheses and Examples of $(N_2)^{2-}$ and $(N_2)^{3-}$ Complexes and Density Functional Theory Comparisons of Closed Shell Sc^{3+}, Y^{3+}, and Lu^{3+} versus $4f^9$ Dy^{3+}. *Inorg. Chem.* **2011**, *50* (4), 1459 1469.
(37) Rinehart, J. D.; Fang, M.; Evans, W. J.; Long, J. R. Strong exchange and magnetic blocking in N_2^{3-} -radical-bridged lanthanide complexes. *Nat. Chem.* **2011**, *3* (7), 538 542.
(38) Rinehart, J. D.; Fang, M.; Evans, W. J.; Long, J. R. A N_2^{3-} Radical-Bridged Terbium Complex Exhibiting Magnetic Hysteresis at 14 K. *J. Am. Chem. Soc.* **2011**, *133* (36), 14236 14239.
(39) MacDonald, M. R.; Bates, J. E.; Fieser, M. E.; Ziller, J. W.; Furche, F.; Evans, W. J. Expanding Rare-Earth Oxidation State Chemistry to Molecular Complexes of Holmium(II) and Erbium(II). *J. Am. Chem. Soc.* **2012**, *134* (20), 8420 8423.
(40) Leconte, N.; Moutet, J.; Constantin, T.; Molton, F.; Philouze, C.; Thomas, F. Coordination Chemistry of the Redox Non-Innocent Ligand Bis(2-amino-3,5-di-tert-butylphenyl)amine with Group 10 Metal Ions (Ni, Pd, Pt). *Eur. J. Inorg. Chem.* **2018**, *2018* (16), 1752 1761.
(41) Shimazaki, Y.; Stack, T. D. P.; Storr, T. Detailed Evaluation of the Geometric and Electronic Structures of One-Electron Oxidized Group 10 (Ni, Pd, and Pt) Metal(II)-(Disalicylidene)diamine Complexes. *Inorg. Chem.* **2009**, *48* (17), 8383 8392.
(42) Shannon, R. Revised effective ionic radii and systematic studies of interatomic distances in halides and chalcogenides. *Acta Crystallogr. Sect. A: Cryst. Phys. Diffr. Theor. Gen. Crystallogr.* **1976**, *32* (5), 751 767.
(43) Manriquez, J. M.; Bercaw, J. E. Preparation of a dinitrogen complex of bis (pentamethylcyclopentadienyl) zirconium (II). Isolation and protonation leading to stoichiometric reduction of dinitrogen to hydrazine. *J. Am. Chem. Soc.* **1974**, *96* (19), 6229 6230.
(44) Sanner, R. D.; Manriquez, J. M.; Marsh, R. E.; Bercaw, J. E. Structure of. mu.-dinitrogen-bis (bis (pentamethylcyclopentadienyl) dinitrogenzirconium (II)),{(h^5-$C_5(CH_3)_5)_2ZrN_2$}N2. *J. Am. Chem. Soc.* **1976**, *98* (26), 8351 8357.
(45) Pool, J. A.; Lobkovsky, E.; Chirik, P. J. Hydrogenation and cleavage of dinitrogen to ammonia with a zirconium complex. *Nature* **2004**, *427* (6974), 527 530.
(46) Bernskoetter, W. H.; Lobkovsky, E.; Chirik, P. J. Kinetics and Mechanism of N2 Hydrogenation in Bis(cyclopentadienyl) Zirconium Complexes and Dinitrogen Functionalization by 1,2-Addition of a Saturated C H Bond. *J. Am. Chem. Soc.* **2005**, *127* (40), 14051 14061.
(47) Brintzinger, H.; Bercaw, J. E. Bis (pentamethylcyclopentadienyl) titanium (II). Isolation and reactions with hydrogen, nitrogen, and carbon monoxide. *J. Am. Chem. Soc.* **1971**, *93* (8), 2045 2046.
(48) de Wolf, J. M.; Blaauw, R.; Meetsma, A.; Teuben, J. H.; Gyepes, R.; Varga, V.; Mach, K.; Veldman, N.; Spek, A. L. Bis-(tetramethylcyclopentadienyl)titanium Chemistry. Molecular Structures of $[(C_5HMe_4)(\ -\eta^1{:}\eta^5\text{-}C_5Me_4)Ti]_2$ and $[(C_5HMe_4)_2Ti]_2N_2$. *Organometallics* **1996**, *15* (23), 4977 4983.
(49) Hanna, T. E.; Bernskoetter, W. H.; Bouwkamp, M. W.; Lobkovsky, E.; Chirik, P. J. Bis(cyclopentadienyl) Titanium Dinitrogen Chemistry: Synthesis and Characterization of a Side-on Bound Haptomer. *Organometallics* **2007**, *26* (9), 2431 2438.
(50) Semproni, S. P.; Milsmann, C.; Chirik, P. J. Side-on Dinitrogen Complexes of Titanocenes with Disubstituted Cyclopentadienyl Ligands: Synthesis, Structure, and Spectroscopic Characterization. *Organometallics* **2012**, *31* (9), 3672 3682.
(51) Coles, M. P.; Hitchcock, P. B.; Khvostov, A. V.; Lappert, M. F.; Li, Z.; Protchenko, A. V. Crystalline amidocerium(IV) oxides and a side-on bridging dioxygen complex. *Dalt. Trans.* **2010**, *39* (29), 6780 6788.
(52) Huh, D. N.; Ziller, J. W.; Evans, W. J. Isolation of reactive Ln(II) complexes with C_5H_4Me ligands (CpMe) using inverse sandwich countercations: synthesis and structure of [(18-crown-6)K(-CpMe)-K(18-crown-6)][CpMe3LnII] (Ln = Tb, Ho). *Dalt. Trans.* **2018**, *47* (48), 17285 17290.

https://dx.doi.org/10.1021/jacs.0c01021
J Am Chem Soc 2020 142 9302 9313